Supplemental Materials

Independent control of reciprocal and lateral inhibition at the axon terminal of retinal bipolar cells

Masashi Tanaka & Masao Tachibana

Department of Psychology, Graduate School of Humanities and Sociology,

The University of Tokyo, Bunkyo-ku, Tokyo 113-0033, Japan

Supplemental figures

Supplemental movie legend

Supplemental movie. Outputs from the array of BC units in response to binominal noise
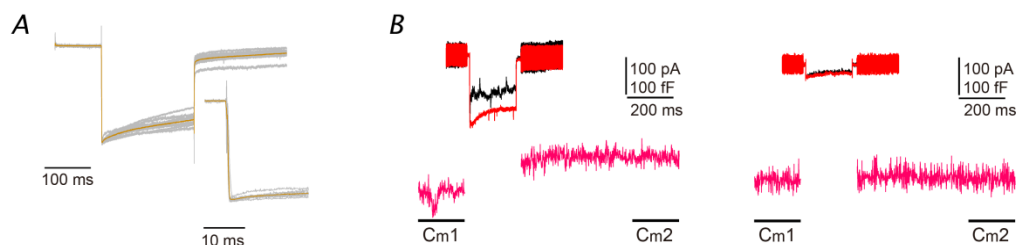

Supplemental references

Supplemental figures

Figure S1. Quantification of the reciprocal IPSC

A, The I_{Ca} template used to quantify the reciprocal IPSC in Fig. 1*A*. To obtain the current responses without IPSC an axotomized terminal was depolarized from −70 to −10 mV for 200 ms in the presence of bath-applied 200 μM picrotoxin and 10 μM strychnine. The first three responses recorded from each cell were averaged and peak normalized (gray traces), and then the averaged traces from 11 terminals were averaged, yielding the I_{Ca} template (orange). We could estimate the reciprocal IPSC in each axotomized terminal (Fig. 1*A*) as the difference between its averaged response and the peak normalized I_{Ca} template. This approach was justifiable for the following reasons. First, the shape of I_{Ca} was similar among 11 terminals, which was confirmed by the relatively small error when the I_{Ca} template was peak normalized to them (the charge of the difference: 0.69 ± 1.86 pC; mean ± SD; n = 11; also see Li et al., 2007). Second, reciprocal IPSCs are unlikely to truncate I_{Ca} peak; the peak of I_{Ca} in control (amplitude: 192.5 ± 8.9 pA; time to peak: 1.55 ± 0.10 ms; n = 47) was not different from that in the presence of bath-applied picrotoxin and strychnine (amplitude: 231.8 ± 27.7 pA, n = 11, P = 0.201, Welch's t-test; time to peak: 1.4 ± 0.6 ms, n = 11, P = 0.835, Welch's t-test). Finally, our estimation of the reciprocal IPSC in Fig. 1*C–D* was largely consistent with previous results (Vigh and von Gersdorff, 2005). The I_{Ca} template contains not only I_{Ca} but also other currents such as Ca^{2+}-activated chloride current (Okada et al., 1995). However, this did not affect the quantification of the reciprocal IPSC because such currents are included both in the I_{Ca} template and in individual traces. The inset shows the expanded traces. **B,** Quantification of the reciprocal IPSC in Fig. 1*B*. Axotomized terminals were depolarized from −70 mV to various membrane potentials. Exemplified individual traces were shown (left: to −30 mV; right: to −40 mV). The reciprocal IPSC was estimated as the difference between the current responses before (black) and during puff-application of 100 μM bicuculline (BIC) and 800 μM TPMPA (red). Q_{Ca} was the charge of the current response during the 200 ms pulse during puff-application. The membrane capacitance (magenta) was obtained by Sine + DC method and ΔC_m was determined as the difference between the averaged capacitance before the stimulus onset (C_m1: from −220 to −20 ms) and that after the stimulus offset (C_m2: from 500 to 700 ms).
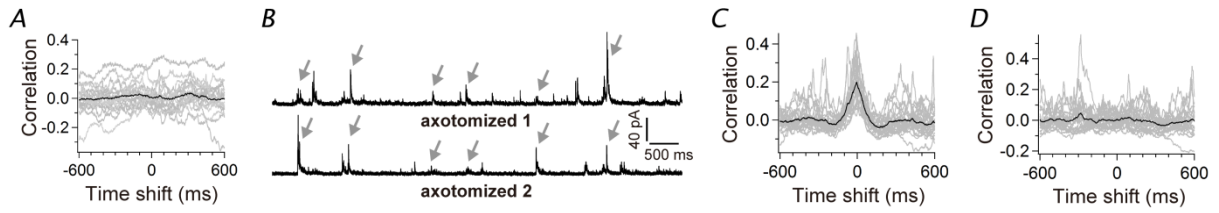
Figure S2. Synchronization of spontaneous IPSCs in axotomized Mb1 BC terminals

A, Shuffled cross-correlograms obtained from the pair shown in Fig. 2*C*. Simultaneously recorded eighteen 5 s segments of current traces were shuffled, and cross-correlograms were calculated from the 18 artificially paired segments. The averaged cross-correlogram was flat (black), indicating the peak of the cross-correlogram observed in Fig. 2*D* could be ascribed to synchronized IPSCs unique to simultaneously obtained recordings. *B,* Spontaneous IPSCs recorded from another pair of nearby (32.3 μm apart) axotomized terminals voltage-clamped at −10 mV (axotomized 1 and 2) as in Fig. 2*C*. Arrows indicate nearly synchronized IPSCs. *C, D,* Cross-correlograms calculated from twenty-four 5 s segments of current traces simultaneously recorded from the pair shown in *B* (*C*, gray) and that calculated from shuffled segments (*D*, gray). Averaged traces are also shown (black).
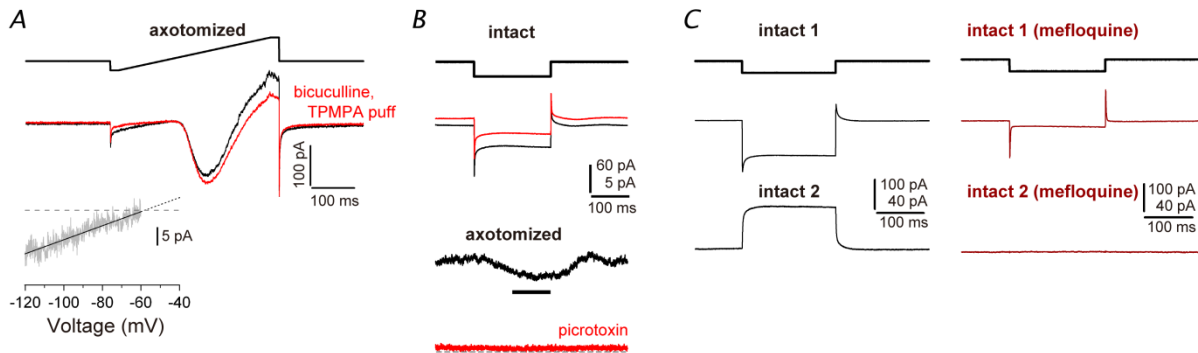
Figure S3. Tonic GABAergic conductance and gap junction conductance

A, Tonic GABAergic conductance. A voltage ramp from −120 to +60 mV (1 mV / ms, interposed between 20 ms plateaus) was applied to an axotomized terminal. The tonic GABAergic current was obtained as the difference between the current responses before (black) and during puff-application of 200 μM picrotoxin or puff-application of 100 μM BIC and 800 μM TPMPA (red). The conductance of the tonic GABAergic current was obtained as the slope of the line (inset, black) fitted to the tonic GABAergic current between −120 and −60 mV (inset, gray). Using this protocol, E_{Cl} was also estimated as the voltage at which the extrapolated line (dotted line) crossed the zero current (broken line). In this case, the conductance of the tonic GABAergic current was 190.5 pS and E_{Cl} was −57.9 mV. **B,** Hyperpolarization of an intact terminal from −70 to −90 mV for 200 ms reduced the tonic outward current in a nearby (18.5 μm apart) axotomized terminal voltage-clamped at −10 mV (black; average of 70 traces). The reduction of the tonic current could not be observed in the presence of bath-applied 200 μM picrotoxin (red; average of 40 traces), showing that the reduced current was GABAergic. The reduction of the tonic GABAergic conductance by hyperpolarization of the intact terminal was 59.6 pS, calculated as $- (I_{hyp} - I_{rest}) / (V_m - E_{Cl})$, where I_{hyp} is the mode of the current recorded for the last 100 ms of the pulse (horizontal black bar) in the axotomized terminal, I_{rest} is the mode of the current for 100 ms just before the pulse, V_m is the holding potential of the axotomized terminal (−10 mV), and E_{Cl} was − 55 mV. To calculate the conductance, at least 40 traces were averaged for each pair. The broken line indicates 0 pA in the axotomized terminal. **C,** Gap junction conductance. When an intact terminal (intact 1) was hyperpolarized from −70 to −90 mV, an outward current through gap junctions was recorded from a nearby (35.0 μm apart) intact terminal voltage-clamped at −70 mV (intact 2). The gap junction conductance was 2.35 nS (left), calculated as $- (I_{hyp} - I_{rest}) / (V_{hyp} - V_{rest})$, where I_{hyp} is the mode of the current recorded from intact 2 during the 200 ms pulse, I_{rest} is the mode of the current in intact 2 for 100 ms just before the pulse onset, V_{hyp} is −90 mV, and V_{rest} is −70 mV. The hyperpolarizing pulse was applied to either terminal of the pair, and the bidirectionally obtained gap junction conductance was averaged to yield the representative of the pair in population analysis. Two hour bath-application of 10 μM mefloquine severely reduced the gap junction conductance obtained similarly from another pair of intact terminals (right; intact 1 and 2, 34.0 μm apart). In this case, the gap junction conductance was 27.9 pS.
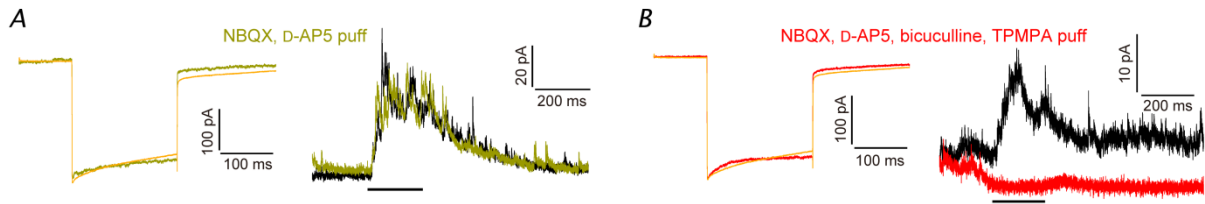
3

Figure S4. Separation protocol of reciprocal and lateral inhibition

A, Effects of puff-applied 10 μM NBQX and 20 μM D-AP5 on reciprocal (left) and lateral inhibition (right). An axotomized terminal was depolarized from −70 to −10 mV for 200 ms (left). The averaged current trace (dark yellow) was similar to the peak normalized I_{Ca} template (orange), showing that the reciprocal IPSC was severely reduced by the puff-application. On the other hand, the lateral IPSC induced in an axotomized terminal voltage-clamped at −10 mV by depolarization of a nearby (44.7 μm apart) intact terminal from −70 to −10 mV for 200 ms (right, black) was not reduced by the puff-application of inhibitors to the intact terminal (dark yellow). **B,** Puff-application of 100 μM BIC and a high concentration of TPMPA in addition to 10 μM NBQX and 20 μM D-AP5 (red) severely reduced both the reciprocal IPSC (left; 200 μM TPMPA) and the lateral IPSC (right; 800 μM TPMPA). The lateral IPSC was recorded from a pair as in *A* (53.1 μm apart), and inhibitors were puff-applied to the recorded axotomized terminal.
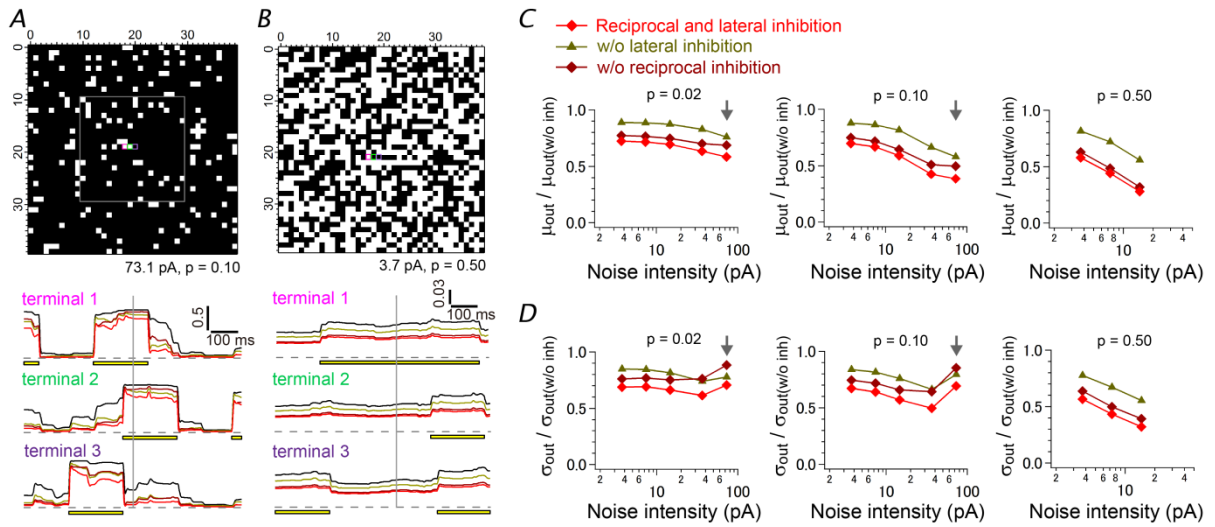
4

Figure S5. Model outputs in response to binominal noise

A, B, Binominal noise of 73.1 pA with the probability of 0.10 (*A*) or that of 3.7 pA with the probability of 0.50 (*B*) was generated every 200 ms in each BC unit. The phase of the noise generation was randomized across BC units (See yellow bars in the lower panel). In the upper panel, the pattern of noise inputs at the timing indicated as the gray vertical line (lower panel) is illustrated. The gray square (*A*, upper panel, 500 × 500 μm) indicates the region where the mean and SD of outputs are calculated in *C* and *D*. In the lower panel, outputs from three exemplified BC units (upper panel; magenta, green, and purple squares) are illustrated for the model (red), the model without any inhibition (black), the model without lateral inhibition (dark yellow), and the model without reciprocal inhibition (dark red). See also Supplemental Movie 1. ***C, D,*** Mean (μ_{out}; *C*) and SD (σ_{out}; *D*) of the outputs in the gray square region in *A* as a function of the intensity and probability of the applied binominal noise (averaged value of 800 ms period). Values in the model (red diamond), in the model without lateral inhibition (dark yellow triangle), and in the model without reciprocal inhibition (dark red diamond) are normalized to that in the model without any inhibition (w/o inh; black traces in *A* and *B*). Arrows indicate the condition under which reciprocal inhibition contributed to noise reduction.

Supplemental movie legend

Supplemental movie. Outputs from the array of BC units in response to binominal noise

Output from BC units in the model based on the experimental results (left) and that without any inhibition (right) in response to binominal noise of 73.1 pA with the probability of 0.10 as in Fig. S5*A*. The background noise is substantially reduced by reciprocal and lateral inhibition, which further contributes to improvement of SNR depending on input patterns. The movie shows the outputs in the scale between 0 (black) and 1 (white) for 400 ms with the frame interval of 10 ms. The frame rate of the movie is 10 frames per second.

Supplemental References

Okada T, Horiguchi H & Tachibana M (1995). Ca^{2+}-dependent Cl^- current at the presynaptic terminals of goldfish retinal bipolar cells. *Neurosci Res* **23**, 297–303.